



저작자표시-비영리-변경금지 2.0 대한민국

이용자는 아래의 조건을 따르는 경우에 한하여 자유롭게

- 이 저작물을 복제, 배포, 전송, 전시, 공연 및 방송할 수 있습니다.

다음과 같은 조건을 따라야 합니다:



저작자표시. 귀하는 원저작자를 표시하여야 합니다.



비영리. 귀하는 이 저작물을 영리 목적으로 이용할 수 없습니다.



변경금지. 귀하는 이 저작물을 개작, 변형 또는 가공할 수 없습니다.

- 귀하는, 이 저작물의 재이용이나 배포의 경우, 이 저작물에 적용된 이용허락조건을 명확하게 나타내어야 합니다.
- 저작권자로부터 별도의 허가를 받으면 이러한 조건들은 적용되지 않습니다.

저작권법에 따른 이용자의 권리는 위의 내용에 의하여 영향을 받지 않습니다.

이것은 [이용허락규약\(Legal Code\)](#)을 이해하기 쉽게 요약한 것입니다.

[Disclaimer](#)

이학석사 학위논문

**Variations of PM₁₀ concentration in
South Korea in response to typhoon
activity in the South China Sea**

남중국해 태풍 활동에 따른 우리나라 PM₁₀ 농도의
변화

2017년 12월

서울대학교 대학원

지구환경과학부

한 여 진

Abstract

This thesis has investigated the relationship between typhoon activity over the western North Pacific and particulate matter $\leq 10 \mu\text{m}$ diameter (PM_{10}) concentration in South Korea. Among all 345 typhoons for the period 2001–2016, 26% of them indicated maximum PM_{10} concentration during life time when they occurred in the South China Sea (SCS; 110°E – 130°E and 10°N – 25°N). For the composite analysis of 219 typhoons passing through the SCS, a tilted Rossby wave like pattern appeared from subtropics (SCS) to high latitudes (the Kamchaka peninsula). In South Korea, anomalous high pressure, shallow boundary layer, and warm air temperature are observed, which are favorable to increase PM_{10} concentration. The Rossby wave-like feature varied according to season and typhoon intensity. The wave amplitude was smaller, and the wave propagated more to South Korea in autumn than in summer. The wave amplitude had stronger when typhoon intensity was stronger, contributing higher PM_{10} concentration in South Korea.

The PM_{10} transboundary transport from Chian is also important contribution to PM_{10} concentration increase in South Korea. Based on 72-hour back trajectories from the HYSPLIT model, the 219 typhoons in the SCS are divided into three types according to source region; local, continental and oceanic types. The local and oceanic types showed similar Rossby wave-like pattern, while in the continental type, a wide low pressure anomaly condition is dominant over South Korea which is hard to be seen as the Rossby wave pattern. The stable condition which can be referred as shallow boundary layer height and warm temperature appear in the local and oceanic type, however, it does not be seen in the continental

type. Mean PM₁₀ concentration of continental type is the highest, followed by local and oceanic type. Finally, among the combination of season, tropical cyclone (TC) intensity, and PM₁₀ source types except the continental type, a group of strong TC in the SCS with local type in autumn shows the largest increase of PM₁₀ concentration (17.2 μg m⁻³ higher than seasonal mean 37.7 μg m⁻³) of 21 typhoons. Therefore, this thesis suggests that the effect of typhoon activity over the SCS on PM₁₀ concentration in South Korea should be considered when we study the variation of the PM₁₀ concentration.

Keywords : PM₁₀ concentration, typhoon, South China Sea, Rossby wave propagation, HYSPLIT model

Student number : 2016-20434

Contents

Abstract	i
Contents	iii
List of Table	iv
List of Figures	v
1. Introduction	1
2. Data and Method	4
3. Results	6
3.1. PM ₁₀ concentration in South Korea vs typhoon activity in the South China Sea	6
3.1.1. <i>Dujuan (2003)</i>	6
3.1.2. <i>Typhoons in the South China Sea</i>	11
3.1.3. <i>Rossby wave-like pattern induced by typhoons</i>	14
3.2. Environmental factors affecting variation of PM ₁₀ concentration	18
3.2.1. Seasonal variations: Summer and autumn.....	18
3.2.2. <i>Typhoon intensity</i>	22
3.2.3. <i>PM₁₀ source type</i>	26
3.2.4. <i>Combination of environmental conditions</i>	32
4. Summary	34
5. Discussion	36
References	37

List of Table

Table 1 Classification of typhoons and the average of maximum PM₁₀ concentration and seasonal PM₁₀ concentration anomaly for each group. Red (Blue) color denotes group of the most PM₁₀ concentration increased (decreased) group.

List of Figures

Fig. 1. (a) Track of typhoon Dujuan (2003) and (b) time series of hourly PM₁₀ concentration and daily precipitation in South Korea.

Fig. 2. Geopotential height anomaly at 500hPa (shading) and wave activity flux (arrow). Scaling for the arrows is given in the right corner of (f) (unit: m² s⁻²). Star-marks indicate daily location of Dujuan.

Fig. 3. (a –c) Arrows denote 1000 hPa daily horizontal winds at 1000 hPa from 31, August to 2, September. (d) 72-h back trajectory at 1000 m and 500 m above ground level in 1, September from Daejeon, produced with HYSPLIT model.

Fig. 4. (a) Locations of 345 typhoons (dot) when maximum PM₁₀ concentration in South Korea is recorded during each typhoon period and percentage density of typhoon location (shading). (b) The climatological typhoon track percentage density from 2001 to 2016. Square area in (a) is the South China Sea (SCS) area and b) indicates the highest density area.

Fig. 5. Composite of geopotential height anomaly at 200 hPa (Φ_{200} , (a)), 500 hPa (Φ_{500} , (b)) and 850 hPa (Φ_{850} , (c)), respectively; 850hPa air temperature (T_{850} , (d)); boundary layer height (e). Dots indicate grids with the 90% statistical significance based on a t-test. Square boxes show the SCS.

Fig. 6. Time series of mean PM₁₀ concentration of 219 typhoons in SCS. Error-bars indicate 95% confidence interval.

Fig. 7. Composite of 500 hPa geopotential height anomaly (Φ_{500} , (a) and (c)); 850 hPa horizontal wind vector (V_{850} , (b) and (d)). The left and right panels are typhoons generated in summer and autumn, respectively. Dots and square boxes ((a) and (c)) indicate grids with the 90% statistical significance based on a t-test

and the SCS area.

Fig. 8. Time series of mean PM_{10} concentration of typhoons in summer (blue line) and autumn (red line). Error-bars indicate 95% confidence interval.

Fig. 9. Composite of 500 hPa geopotential height anomaly (Φ_{500} , (a) and (c)); Boundary layer height ((b) and (d)). The left and right panels are strong intensity typhoons and weak intensity typhoons, respectively. Dots and square boxes ((a) and (c)) indicate grids with the 90% statistical significance based on a t-test and the SCS area.

Fig. 10. Time series of mean PM_{10} concentration of weak intensity typhoons (blue line) and strong intensity typhoon (red line). Error-bars indicate 95% confidence interval.

Fig. 11. 72-h back trajectory in 1000 m from surface, originating in Deajeon, produced by HYSPLIT model a). Classification of source region type b).

Fig. 12. Composite of 500 hPa geopotential height anomaly (Φ_{500} (a), (d) and (g)), the boundary layer height ((b), (e) and (h)) and anomaly 850 hPa air temperature (T_{850} , (c), (f) and (i)). The left, middle, and right panels are the local, oceanic, and continental type, respectively. Dots indicate grids with the 90% statistical significance based on a t-test. Square boxes indicate the SCS.

Fig. 13. Time series of mean PM_{10} concentration of typhoons for local source type (red line), the continental type (orange line) and the oceanic type (blue line). Error-bars indicate 95% confidence interval.

1. Introduction

The particle matters smaller than $10\mu\text{m}$ in diameter, so called PM_{10} , is one of the air pollutants causing serious problem on human health and environment. According to previous reports, increasing number of asthma and chronic obstructive pulmonary disease patient is related to the increasing number of high PM_{10} concentration events (MacNee et al., 2003; Mercedes et al., 2006). PM_{10} could reduce visibility (Zhao et al., 2013) and leaves stain and dirt on buildings (Wang et al., 2002). As these problems exacerbate as the PM_{10} concentration increases, it is necessary to understand mechanisms of PM_{10} concentration increase. Especially, this study focuses on South Korea which was located under strong westerly and in the east of China continent, faces to various mechanisms that enrich the PM_{10} concentration.

Interestingly, however, according to numerous studies that conducted abroad, air pollution could be severely worse under the influence of typhoon activity (Huang and Fung, 2005; Feng et al., 2007; Wang et al., 2008; Fang et al., 2009; Yang et al., 2012; Wu et al., 2013; Jiang et al., 2015; Yan et al., 2016; Lam et al., 2018). Feng et al. (2007) reported that typhoon MELOR (2004) constructed large subsidence motion in its vicinity and thus weak wind and low boundary layer condition are created over the Pearl River Delta region to increase PM_{10} concentration up to $400\ \mu\text{g m}^{-3}$ in daily average. Yang et al. (2012) also mentioned that typhoon may cause a horizontal aerosol transport during which PM_{10} concentration in Hong Kong is reported six times higher than usual. In addition, following climatological analysis of typhoon activity influence on PM_{10} and other air pollutants is conducted continuously (Yan et al., 2016; Lam et al., 2018).

In case of South Korea, study about the relationship between typhoon activity and PM_{10} concentration is not fully investigated. Jeon (2011) which investigated typhoon influence on PM_{10} concentration in Busan, South Korea explained sudden PM_{10} episode as a low boundary layer, a horizontal PM_{10} transport and a resuspension of surface dust induced by typhoon USAGI (August, 2007) and NARI (September, 2007). Even so, Jeon (2011) studied in regional scale and with the above mechanism, it is hard to fully explain typhoon influence on South Korea. The other studies (Kim, 2009; Lee et al., 2013) also are case study researches and mostly deal with direct effect of typhoon on PM_{10} concentration increase.

However, it is necessary to consider not only direct effect, but also indirect effect of typhoons throughout the western North Pacific. Nitta (1987) said convective system in the tropical western Pacific that can be considered as typhoon may result anomalous hot days in Japan by generating Pacific Japan (PJ) pattern through Rossby wave propagation (Kawamura and Ogasawara, 2006). Likewise, PJ pattern around Japan induced by typhoon that is located near Philippine Sea intensifies moisture advection at the low level in the coastal region of mainland of Japan which brings heavy rainfall (Kawamura and Ogasawara, 2006; Kosaka et al., 2011). These studies imply that typhoons might modulate the synoptic pattern and weather of mid-latitude even though typhoons are located far from the study region. In this regard, whole typhoons generated in the western North Pacific should be considered.

The objective of this study is the investigation of climatological relationship between PM_{10} concentration increase in South Korea and typhoon activity in the western North Pacific. First of all, the typhoons that influence on the PM_{10} concentration increase in South Korea are searched. Secondly, a mechanism that

typhoons affect PM_{10} concentration increase is explained. Finally, by a classification of typhoon cases according to diverse background conditions and standards, the most favorable conditions of PM_{10} concentration increase related to typhoon activity are analyzed.

2. Data and Method

In this study, one-hour interval PM_{10} data from the Korea Environment Corporation (KECO) is used in the period of 2001–2016. The 6-hour averaged PM_{10} concentration of 271 city-observations defined as a representative South Korea PM_{10} concentration. Typhoon location, intensity and time information in every 6-hour interval are retrieved from the International Best Track Archive for Climate Stewardship (IBTrACS) best track data of Regional Specialized Meteorological Centers-Tokyo Typhoon Center (RSMC). Daily meteorological data about geopotential height, temperature and horizontal and vertical wind speed are obtained from the National Centers for Environmental Prediction reanalysis 2 (NCEP2) with the longitude-latitude resolution of $2.5^{\circ} \times 2.5^{\circ}$. Daily boundary layer height is obtained from the interim version of European Centre for Medium-Range Weather Forecasts (ECMWF) Re-Analysis (ERA-interim) data with the resolution of $1.5^{\circ} \times 1.5^{\circ}$. The ground station meteorological data for 76 stations in South Korea is provided by Korea Meteorological Administration (KMA).

Yellow dust day information is provided from Korea Meteorological Service (KMS). To surely ignore the yellow dust effect, yellow dust days are redefined as additional 3 days before and after each yellow dust day. In case of typhoon whose period is overlapped with newly defined yellow dust period is excluded in this analysis. From 2001 to 2016, 345 typhoons are selected after excluding typhoons that are duplicated.

To look into the factors for increased PM_{10} concentration, the 72-hour back trajectory from the moment that maximum PM_{10} concentration is recorded is calculated by Hybrid Single-Particle Lagrangian Integrated Trajectory model

(HYSPLIT). The arrival point is Deajeon (36.3°N, 127.4°E) which is considered as the center of South Korea. The arrival levels are above 500 m and 1000 m from ground level (Lee et al., 2011, Lee et al., 2013). Potential temperature, mixing depth, relative humidity and terrain height information which are considered as meteorological condition along the trajectory.

3. Results

3.1. PM₁₀ concentration in South Korea vs typhoon activity in the South China Sea

3.1.1. *Dujuan* (2003)

Typhoon *Dujuan* (2003) is 13th typhoon of the 2003 Pacific typhoon. It was generated in the east of the Philippine Sea at late 27th, April and disappeared when it was located in Southern China continent at 3rd, September (Track of *Dujuan*; Fig. 1a). It recorded 150 km h⁻¹ of maximum wind speed when it was just located in south of Taiwan at 1st, September. It was the strongest typhoon in 13 years since typhoon *Hope* in 1979 that struck the Pearl River delta region and it caused many casualties and massive financial damage in Taiwan, Hong Kong, Shenzhen and Guangdong. During the activity period of *Dujuan*, PM₁₀ concentration in South Korea decreased due to the scavenging effect when a high amount of precipitation was recorded (Lim et al., 2012). The 6-hour mean PM₁₀ concentration in Chungbuk recorded a maximum value by 83.1 µg m⁻³ at 1st, September.

In geopotential height anomaly field during the typhoon period (Fig. 2), a center of anomalous high pressure was located over South Korea. It seemed to move eastward from 26th to 28th, August (not shown), in the south of South Korea, however, after 29th, August, as the typhoon became stronger and moved westward in the Western North Pacific (WNP), center of high pressure also moved westward and it stopped over South Korea and remained for six days (Fig. 2). The favorable synoptic condition to accumulate PM₁₀ is a stable condition with light wind and under anomalous high pressure condition (Lee et al., 2013; Oh et al., 2015). The 1000 hPa horizontal wind fields show calm condition over South Korea (Fig. 3a –

c). According to the 72-h back trajectory result produced by HYSPLIT, the back trajectory remains around South Korea in the level of 500m and 1000m from surface (Fig. 3d). It indicates that calm meteorological condition to accumulate PM_{10} concentration in South Korea is constructed for several days from 31th, August.

The dipole-like synoptic pattern is like a structure of Pacific Japan (PJ) pattern (Nitta, 1987; Kosaka and Nakamura, 2006). According to the papers that studied the PJ pattern, high pressure system is widely created over the Korean peninsula and Japan by the Rossby wave propagation from convective activities in the Philippine Sea. In case of the Dujuan, a wave activity flux defined by Takaya and Nakamura (2001) in Fig. 2a –f points the center of high pressure anomaly over South Korea and it is stronger when intensity of Dujuan is stronger. It implies that the stagnation of anomalous high pressure system over South Korea is partially influenced by the Rossby wave propagation from the typhoon, Dujuan.

Under the considerations of the typhoon location which induces the PJ pattern (known as the Philippine Sea) and the Dujuan, typhoons that are located in the South China Sea and the Philippine Sea (SCS; 110°E –130°E and 10°N –25°N) are investigated. The typhoons which are located in the SCS are considered as possible factors that can influence on the generation of favorable meteorological condition to accumulate PM_{10} concentration in South Korea. Among the 345 typhoon cases that are not overlapped by the yellow dust season from 2001 to 2016, the 219 typhoons passed through the SCS. The meteorological conditions around South Korea when the 219 typhoons are located in SCS are investigated using composite analysis.

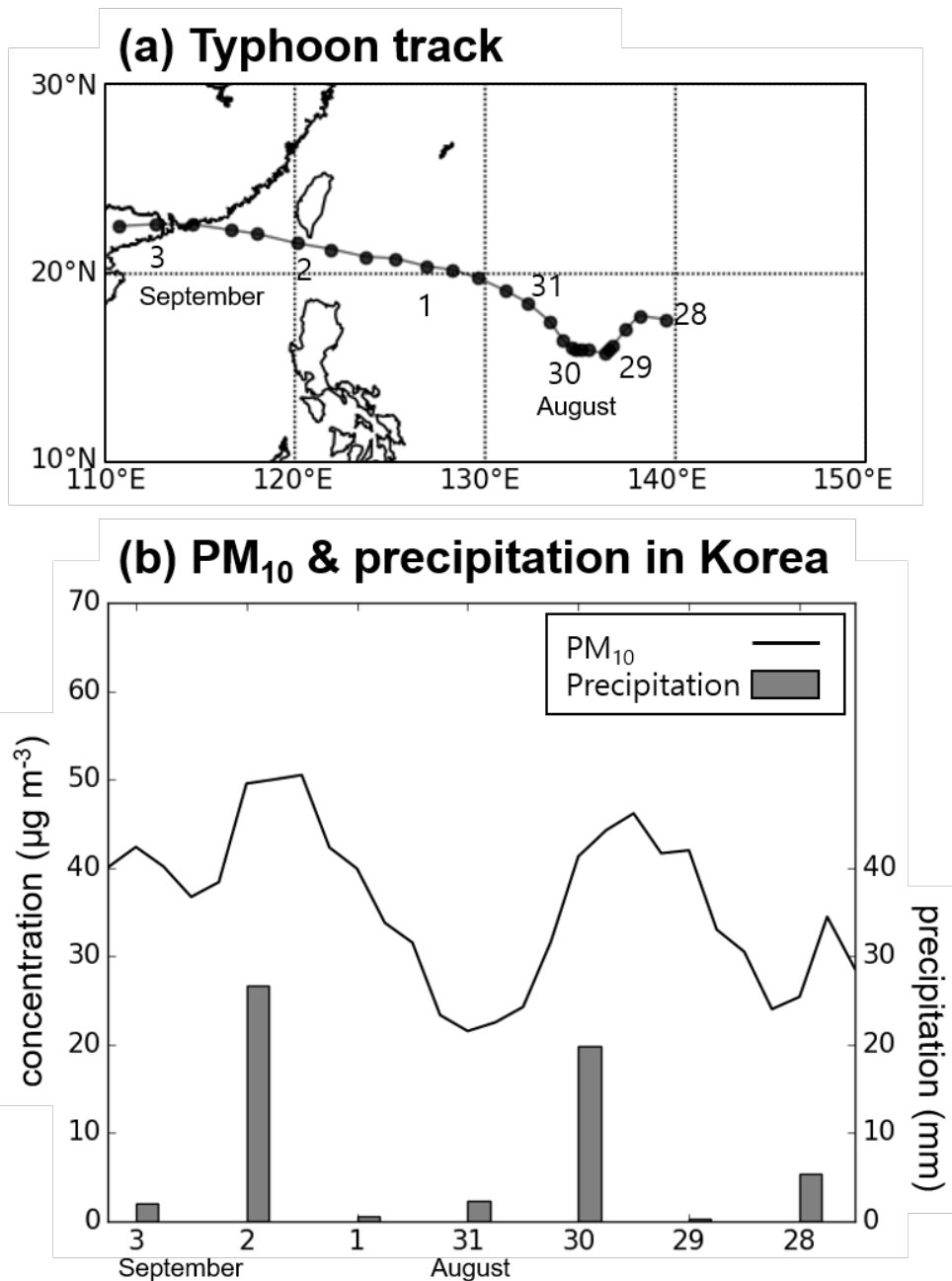


Fig. 1. (a) Track of typhoon Dujuan (2003) and (b) time series of hourly PM₁₀ concentration and daily precipitation in South Korea.

Φ_{500} & wave activity flux

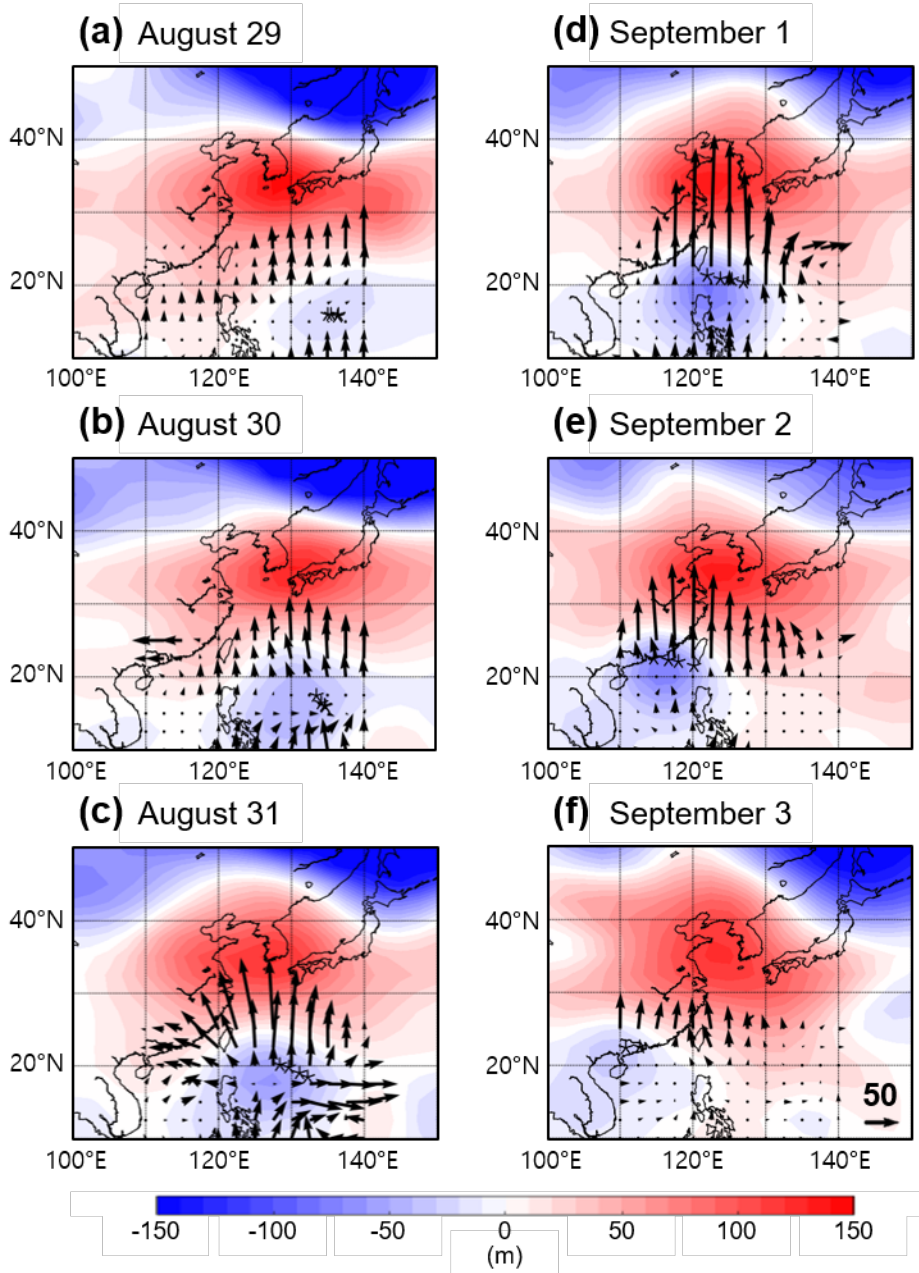


Fig. 2. Geopotential height anomaly at 500hPa (shading) and wave activity flux (arrow). Scaling for the arrows is given in the right corner of (f) (unit: $\text{m}^2 \text{s}^{-2}$). Star-marks indicate daily location of Dujan.

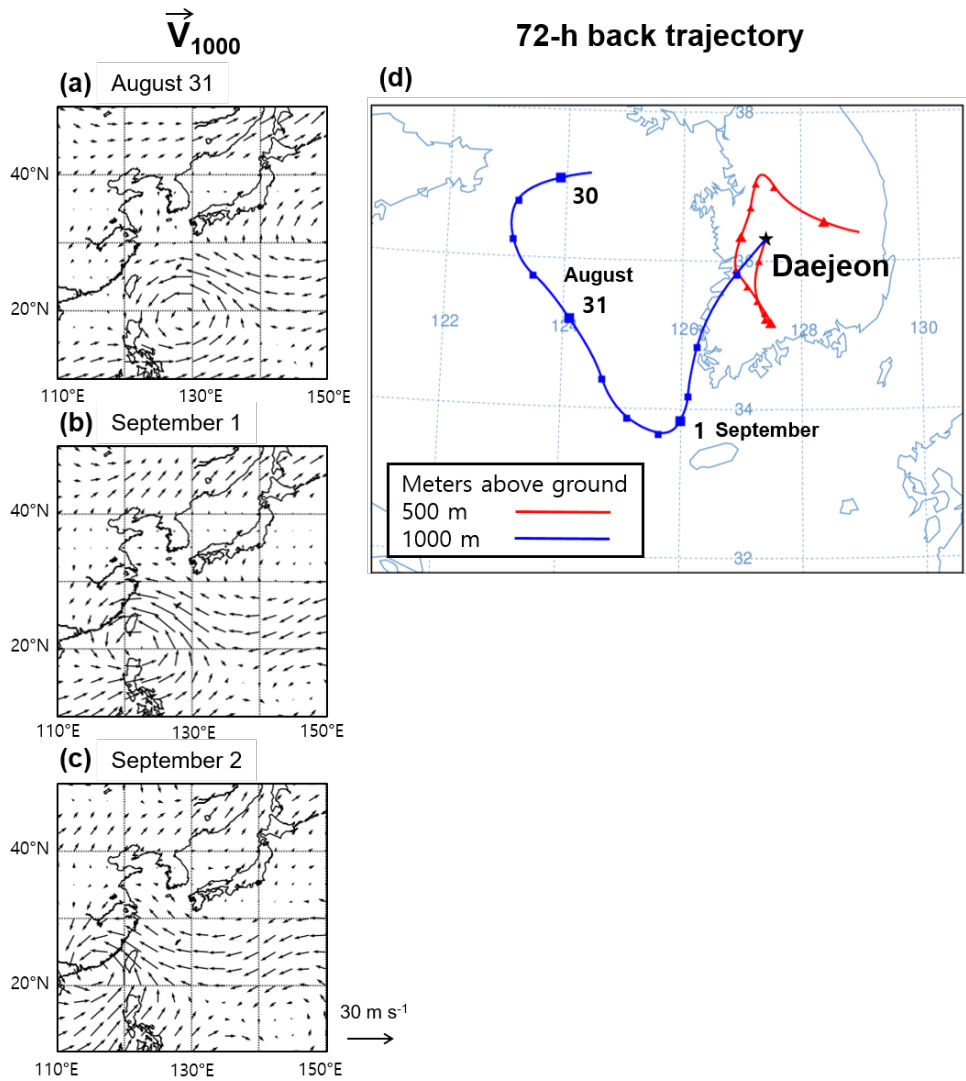


Fig. 3. ((a) –(c)) Arrows denote 1000hPa daily horizontal winds at 1000 hPa from August 31 to September 2. (d) 72-h back trajectory at 1000 m and 500 m above ground level at September 1 from Daejeon, produced with HYSPLIT model.

3.1.2. Typhoons in the South China Sea

The maximum PM₁₀ concentration in South Korea during active period of the Dujuan is recorded when the Dujuan is located in the SCS. The locations where the maximum PM₁₀ concentration in South Korea recorded in each typhoon period are analyzed (Fig. 4a). Among the 345 typhoons, 72% (248) of typhoons show of the 6-hour average maximum PM₁₀ concentration more than 50 $\mu\text{g m}^{-3}$ of typhoons are recorded and 26% (91) of typhoons show that more than 80 $\mu\text{g m}^{-3}$, and 11% (38) of typhoons that more than 100 $\mu\text{g m}^{-3}$. The 175 typhoons account for 58% show of PM₁₀ concentration increase of more than 30 $\mu\text{g m}^{-3}$ within 100-hour before the maximum PM₁₀ concentration. Among them, the 58 typhoons show more than 200% of the PM₁₀ concentration increasing rate.

Using a track density calculation method from Choi et al. (2016), the density of the maximum locations of typhoons are calculated. The most highest density region is seen in area which contains the South China Sea and the Philippine Sea. The region is simply referred to as SCS (110°E –130°E and 10°N –25°N) hereafter. The Philippine Sea area that is included in the SCS are known as the location of typhoon that is associated with the PJ pattern.

The climatological highest density region of typhoon track from 2001 to 2016 is the Philippine Sea and the Western North Pacific (WNP) (Square area in Fig. 4b). Additionally, it is spread toward the north compared to the maximum PM₁₀ concentration location of typhoon. The highest density regions in the both are clearly different each other. This difference may indicate that the typhoons located in the SCS significantly could give an influence on PM₁₀ concentration increase in South Korea.

The 219 typhoons that account for 63.5% of total typhoons are passed through the SCS area from 2001 to 2016. Therefore, through the composite analysis of 219 typhoons for diverse meteorological conditions around South Korea, a role of typhoon activity in the SCS that gives an influence on PM_{10} concentration change in South Korea is investigated.

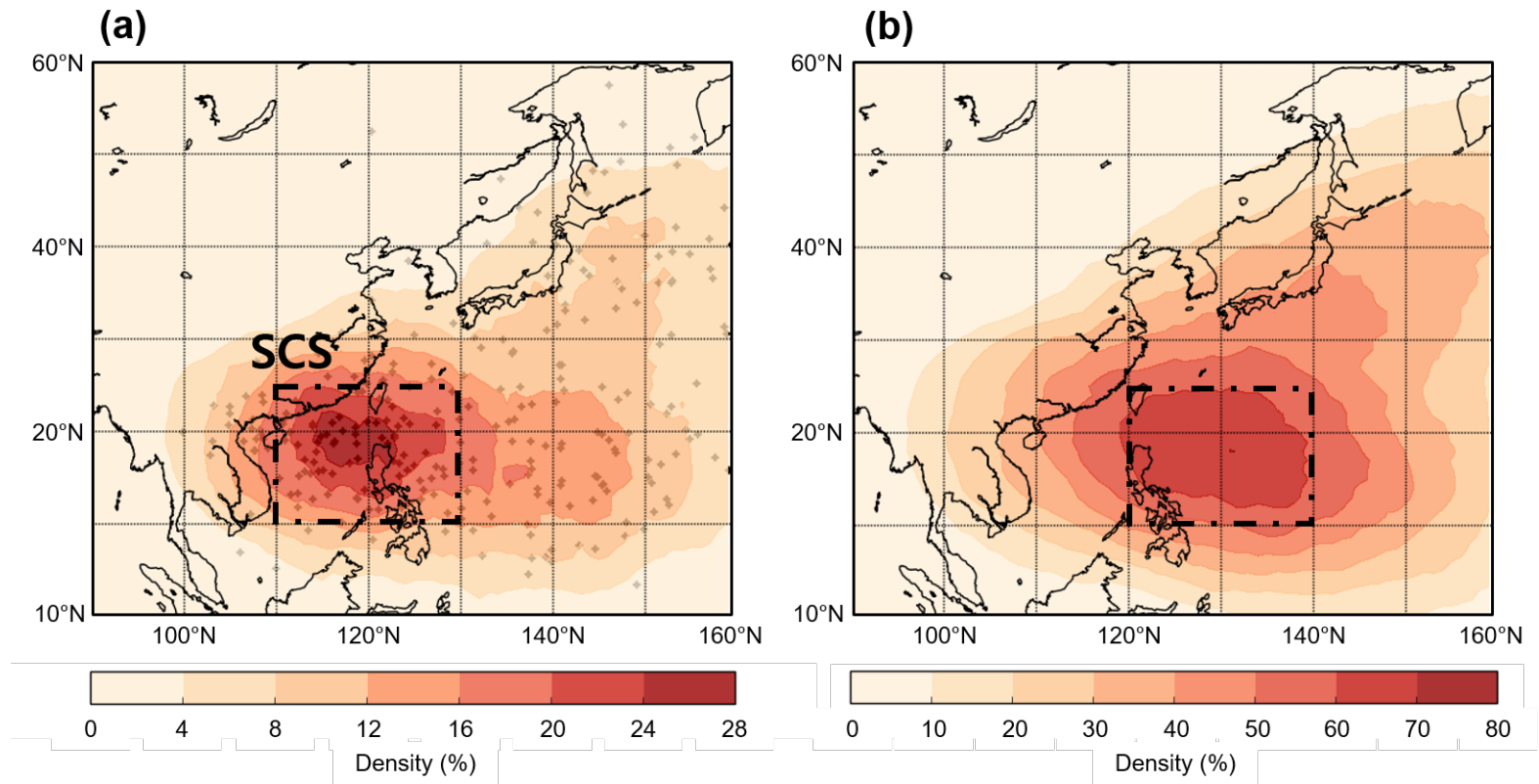


Fig. 4 (a) Locations of 345 typhoons (dot) when maximum PM_{10} concentration in South Korea is recorded during each typhoon period and percentage density of typhoon location (shading). (b) The climatological typhoon track percentage density from 2001 to 2016. Square area in (a) is the South China Sea (SCS) area and b) indicates the highest density area.

3.1.3. Rossby wave-like pattern induced by typhoons

To investigate the influence of typhoons in SCS on PM₁₀ concentration increase in South Korea, we analyze the composite results of meteorological factors which are related to the PM₁₀ concentration (Lee et al., 2011). In the geopotential height anomaly composite fields (Fig. 5a –c), a vertically northeastern tilted Rossby wave-like wave train that propagates from the SCS to the Kamchatka peninsula appears. The high pressure system over South Korea in the wave train resembles that of the PJ pattern which has been mostly located over Japan (Nitta. 1987; Kurihara and Tsuyuki. 1987; Kosaka and Nakamura. 2006). However, the SCS region which includes the west region of the Philippine Sea from the typhoon region of the PJ pattern is different with the South China Sea. Additionally, the high pressure anomaly system over South Korea is also shifted to the west compared to that of the previous PJ pattern studies. Although the location of the wave train is a little bit shifted to the west. According to the Kurihara and Tsuyuki (1987), the high pressure anomaly system induced by convective system in tropical western Pacific has northward tilted structure with height. In this regard, the high pressure anomaly system over South Korea is constructed by the propagation of the Rossby wave induced by typhoons in the SCS.

The high pressure anomaly over South Korea is favorable condition to stagnate the PM₁₀ concentration. Lee et al. (2011) reported that the composite field of 500hPa geopotential height for high-PM₁₀ episode days strong high pressure anomaly over South Korea (Rost and Holst., 2009; Lee et al., 2013; Oh et al., 2015). The stable condition can be also in associating with low boundary layer height anomaly over South Korea (Fig. 5e). Additionally, significantly positive air temperature anomaly over South Korea is another favorable condition to aerosol

formation and chemical reaction (Van Der Wal and Janseen. 2000) (Fig. 5d).

The average PM₁₀ concentration before and after 78-hour from maximum PM₁₀ concentration (zero hour) for 219 typhoons is shown in Fig. 6. As further away from the zero hour, PM₁₀ concentration declines from the maximum PM₁₀ concentration 54.5 $\mu\text{g m}^{-3}$ to 36.4 $\mu\text{g m}^{-3}$. It implies that the PM₁₀ concentration in South Korea experiences an incline when typhoon is located in the SCS.

The Rossby wave-like wave propagation due to the typhoons in tropical western Pacific has been known to be dependable to the seasons and the intensity of typhoon (Nitta, 1987; Yamada and Kawamura, 2007). Also, PM₁₀ concentration is modulated not only by the meteorological conditions, but also by source regions. Therefore, the further composite analysis is proceeded by comparing groups of typhoons according to the different seasons, intensity of typhoon and source region types using HYSPLIT model.

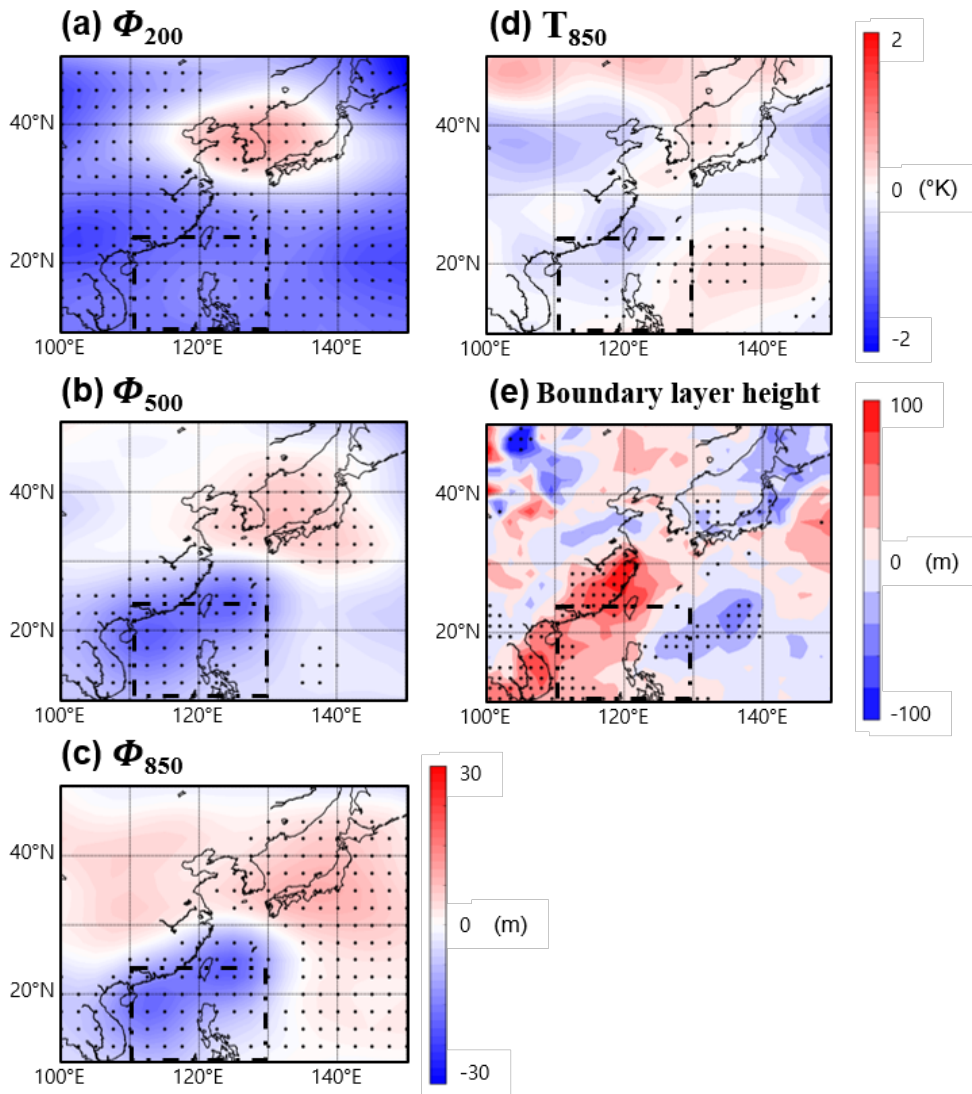


Fig. 5. Composite of geopotential height anomaly at 200 hPa (Φ_{200} , (a)), 500 hPa (Φ_{500} , (b)) and 850 hPa (Φ_{850} , (c)), respectively; 850hPa air temperature (T_{850} , (d)); boundary layer height (e). Dots indicate grids with the 90% statistical significance based on a t-test. Square boxes denote the SCS.

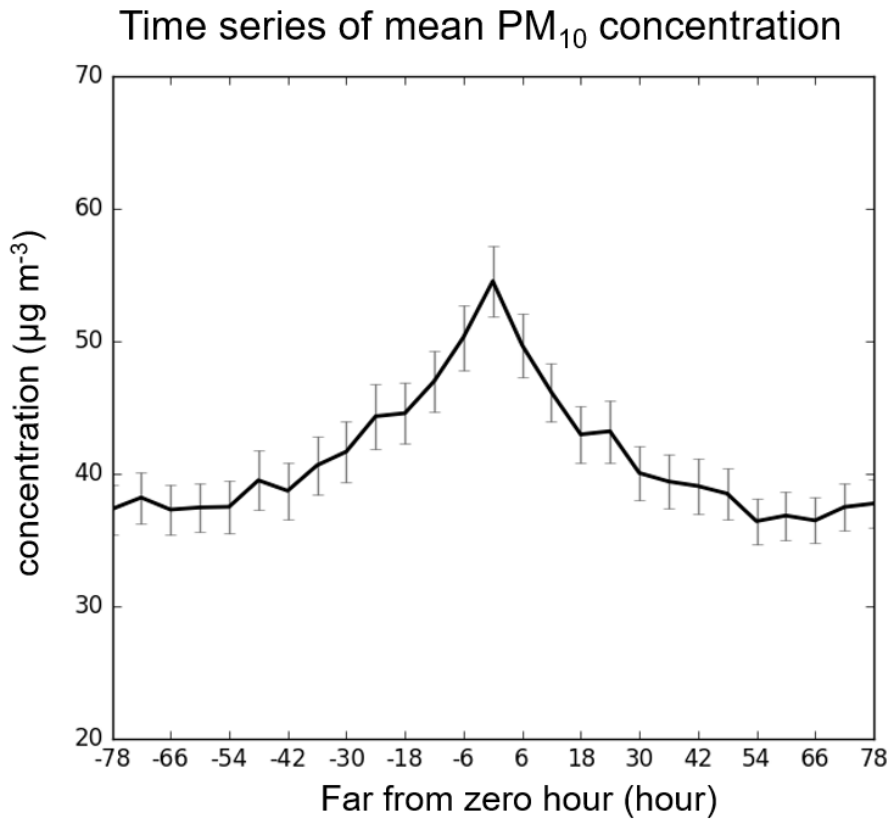


Fig. 6. Time series of mean PM₁₀ concentration of 219 typhoons in SCS. Error-bars indicate 95% confidence interval.

3.2. Environmental factors affecting variation of PM₁₀ concentration

3.2.1. Seasonal variations: Summer and autumn

The wave propagation is closely dependable to seasonal characteristics. According to Yamada and Kawamura. (2007), the wave train formation is dominant in summer season because of the monsoon circulation that guides wave train toward north. On the other hand, in autumn, the monsoon current disappears and another circulation, upper-level Asian jet, guides the Rossby wave propagation to occur hardly. Moreover, typhoon is generated mainly in summer and autumn, and a typhoon season is also set by July –October (Kim et al., 2015). For this reason, typhoon dominant period, summer and autumn is mainly investigated. Among the 219 typhoons passing through the SCS, 198 typhoons (90.4%) are generated in summer (109 typhoons, 49.8%) and autumn (98 typhoons, 44.7%). In this regard, seasonal analysis is focused on the two season, summer and autumn.

The amplitude of the 500 hPa wave train in summer (Fig. 7a) is clearer than that in autumn (Fig. 7b). The high pressure anomaly of wave train is located over South Korea, which seemingly resembles total composite result (Fig. 5b). According to numerous studies related to the PJ pattern (Nitta, 1987; Kurihara and Tsuyuki, 1987; Kawamura and Ogasawara, 2006; Kosaka et al., 2011), favorable conditions to the PJ pattern are satisfied mainly in summer. As the seasonal favor of the PJ pattern, the high pressure anomaly system may due to the influence of the Rossby wave propagation, and may be not in autumn.

In the composite of 850 hPa horizontal wind field in summer, the wind from the south in South Korea, which is referred as monsoon circulation, is dominant (Fig.

7c), which is not expected to transport PM₁₀ aerosols to increase the PM₁₀ concentration in South Korea. In case of autumn, the westerly winds are seen over South Korea (Fig. 7d) which may be expected to get PM₁₀ aerosol from higher PM₁₀ concentration region. Therefore, according to the difference of the composite of 850 hPa wind between summer and autumn, it is expected that the maximum PM₁₀ concentration associated with typhoons in summer are related to the Rossby wave propagation which is generated by the typhoons in the SCS. On the other hand, in autumn, a PM₁₀ transport from the western continent may be expected.

Organizing the maximum PM₁₀ concentration to a zero hour, the time series of mean PM₁₀ concentration before and after 78-hour shows a continuous decline in both summer and autumn season (Fig. 8). In case of summer, the mean PM₁₀ concentration in zero hour increases 31.2 $\mu\text{g m}^{-3}$ at 72-hour before the zero hour to 50.6 $\mu\text{g m}^{-3}$ at the zero hour. On the other hand, in case of autumn, the mean PM₁₀ concentration goes up from 35.3 $\mu\text{g m}^{-3}$ at 72-hour before the zero hour to 55.9 $\mu\text{g m}^{-3}$ at the zero hour. During the entire period, the PM₁₀ concentration in autumn is higher than that in summer. However, seasonal mean value of the PM₁₀ concentration in summer and autumn are 45.2 $\mu\text{g m}^{-3}$ and 37.7 $\mu\text{g m}^{-3}$, respectively. As shown in this analysis when typhoon is located in the SCS area, the PM₁₀ concentration in autumn over South Korea is much higher than that in summer.

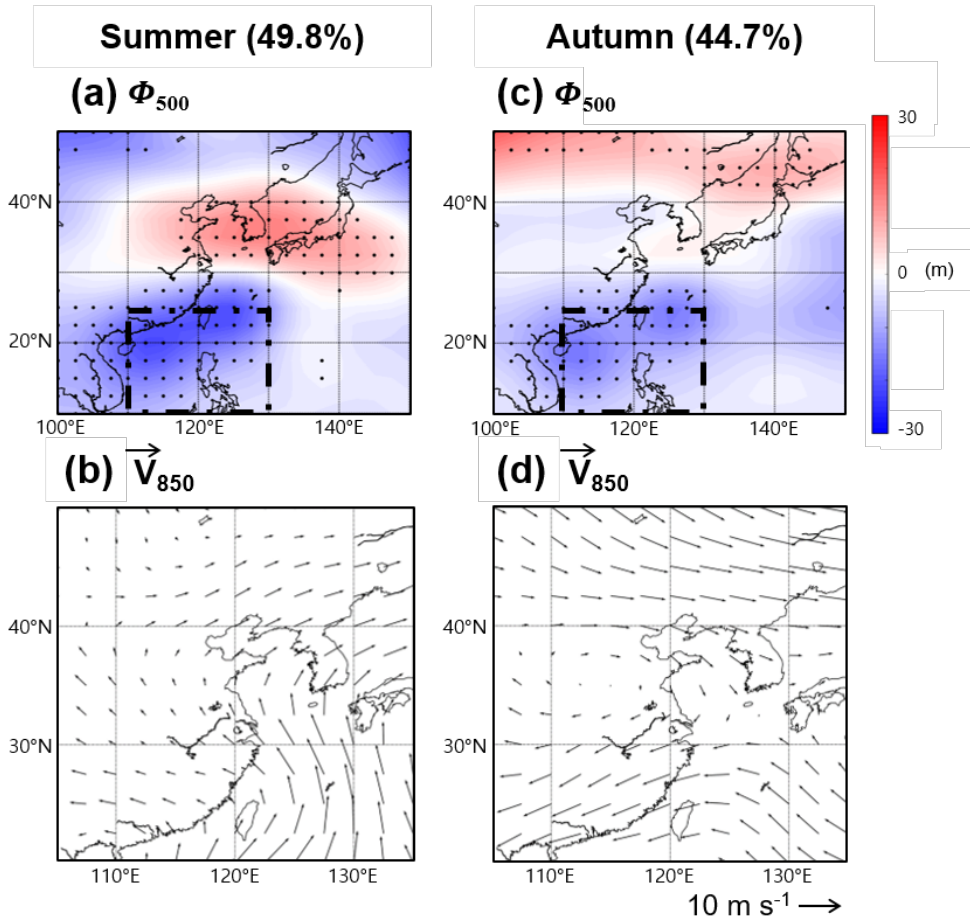


Fig. 7. Composite of 500hPa geopotential height anomaly (Φ_{500} , (a) and (c)); 850hPa horizontal wind vector (\vec{V}_{850} , (b) and (d)). The left and right panels are typhoons generated in summer and autumn, respectively. Dots and square boxes ((a) and (c)) indicate grids with the 90% statistical significance based on a t-test and the SCS area.

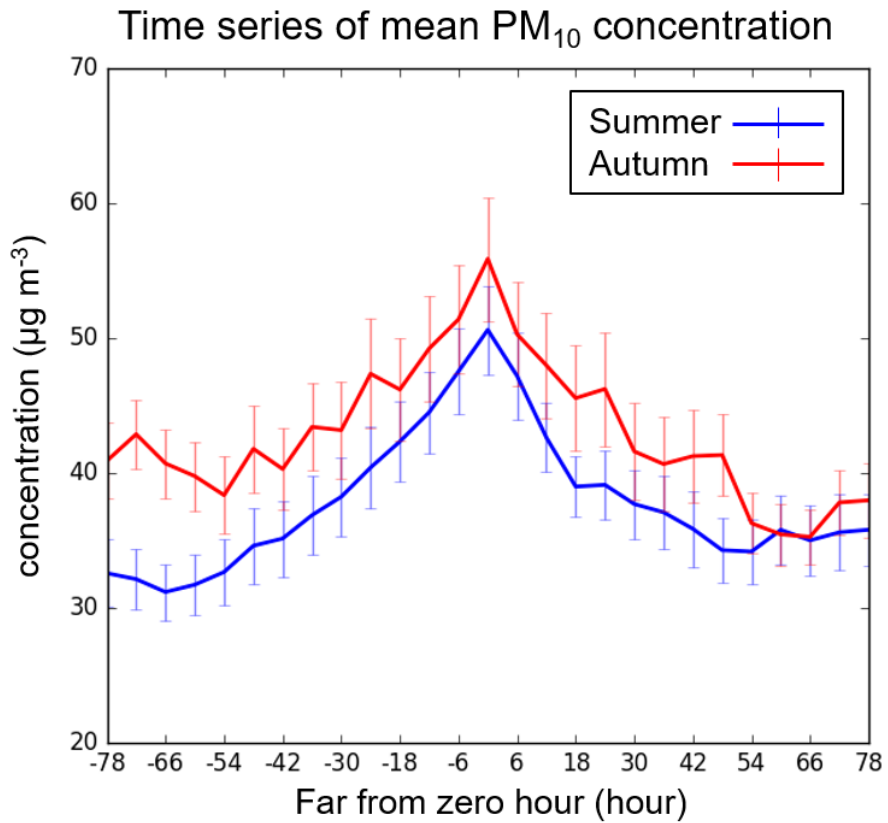


Fig. 8. Time series of mean PM₁₀ concentration associated with typhoons in summer (blue line) and autumn (red line). Error bars indicate 95% confidence interval.

3.2.2. *Typhoon intensity*

The Rossby wave propagation is known to be dominant in mid-summer due to high sea surface temperature of Philippine Sea and the favorable background condition is formed by the monsoon circulation to make easy to propagate the Rossby wave (Nitta, 1987; Yamada and Kawamura, 2007). However, Yamada and Kawamura (2007) reported that the coexistence frequency of the typhoon and wave train is higher in autumn than summer because the high intensity typhoons are more often generated in autumn. According to these, the classification by the maximum intensity of typhoon in its life time is conducted based on the standard of the typhoon level by Saffir-Simpson. The strong typhoon group is defined as a typhoon group that has more than 64 knots of center wind speed.

The 126 typhoons (57.5%) are classified into strong typhoon group and the other 93 typhoons (42.5%) belong to the weak typhoon group. As a result, in case of strong typhoon group, the composite result of geopotential height anomaly at 500 hPa (Fig. 9a) shows the Rossby wave-like wave pattern. On the other hand, in case of the weak typhoon group, the Rossby wave-like wave pattern is not clear (Fig. 9b). For the reason of strong amplitude of wave train in strong typhoon group, South Korea is under a condition of high pressure anomaly, which is one of favorable conditions for a stagnation of PM₁₀.

In a composite of boundary layer height anomaly (Fig. 9c –d), significantly low boundary layer height is seen around South Korea in the strong typhoon group. It implies that the stable condition around South Korea may occur when typhoons are located in the SCS (Fig. 9c). However, the boundary layer height in weak group is not significant around South Korea. Therefore, the strong typhoon in the SCS is favorable to propagate the Rossby wave toward South Korea and to generate

anomalous high pressure condition that makes the state of anomalous low boundary layer height.

According to time series of average PM_{10} concentration in Fig. 10, although error bars of 95% confidence interval in both groups are mostly overlapped for each hour, the mean PM_{10} concentration of the strong typhoon group is higher than that of the weak typhoon group in entire period only except after 60-hour from zero hour. This analysis result implies that typhoon intensity may influence on PM_{10} concentration in South Korea.

The above two groups depend on the season. For the strong typhoon group, 52 typhoons and 62 typhoons are generated in summer and autumn, respectively, which account for 41.3% and 49.2%. Additionally, in case of the weak typhoon group, 54 typhoons and 30 typhoons are occurred in summer and autumn which account for 58.1% and 32.3%, respectively. According to the analysis in 3.2.1, it is found that the Rossby wave propagation produced by typhoon is weakened in autumn. However, in the strong typhoon group which Rossby wave train is more clear than in the weak typhoon group, the number of typhoon cases that are generated in autumn are much more than that in summer. This result implies that, when typhoon intensity in the SCS is stronger, the Rossby wave propagates better than when the weak intensity typhoon is located in the SCS.

Strong group (57.5%)

Weak group (42.5%)

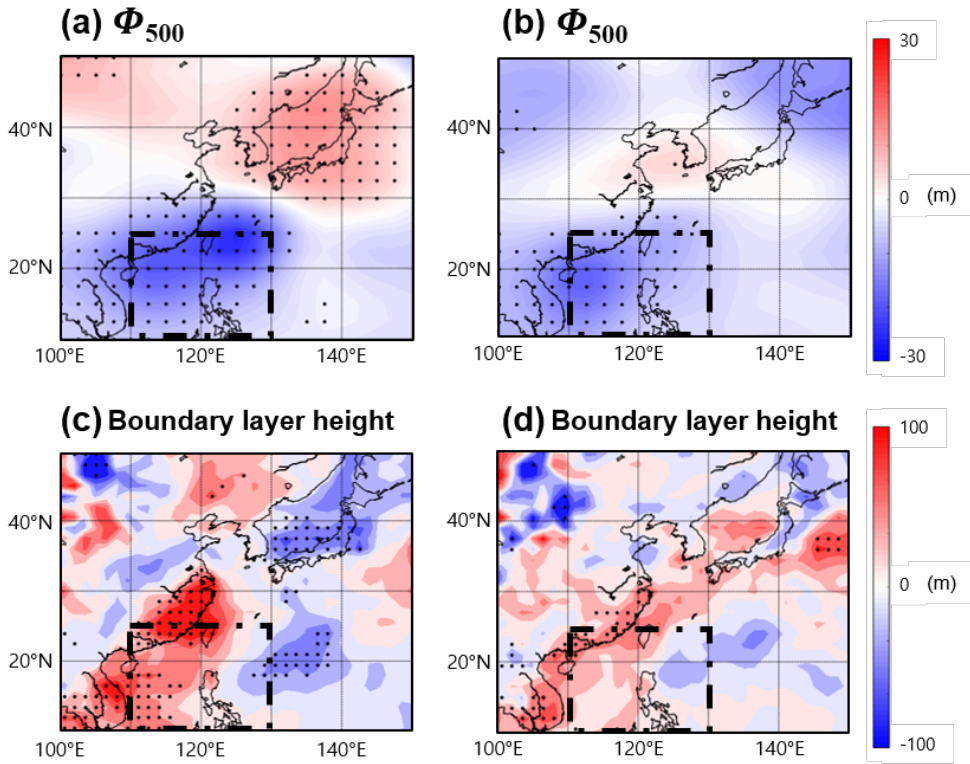


Fig. 9. Composites of 500hPa geopotential height anomaly (Φ_{500} , (a) and (c)); Boundary layer height ((b) and (d)). The left and right panels are strong intensity typhoons and weak intensity typhoons, respectively. Dots and square boxes ((a) and (c)) indicate grids with the 90% statistical significance based on a t-test and the SCS area.

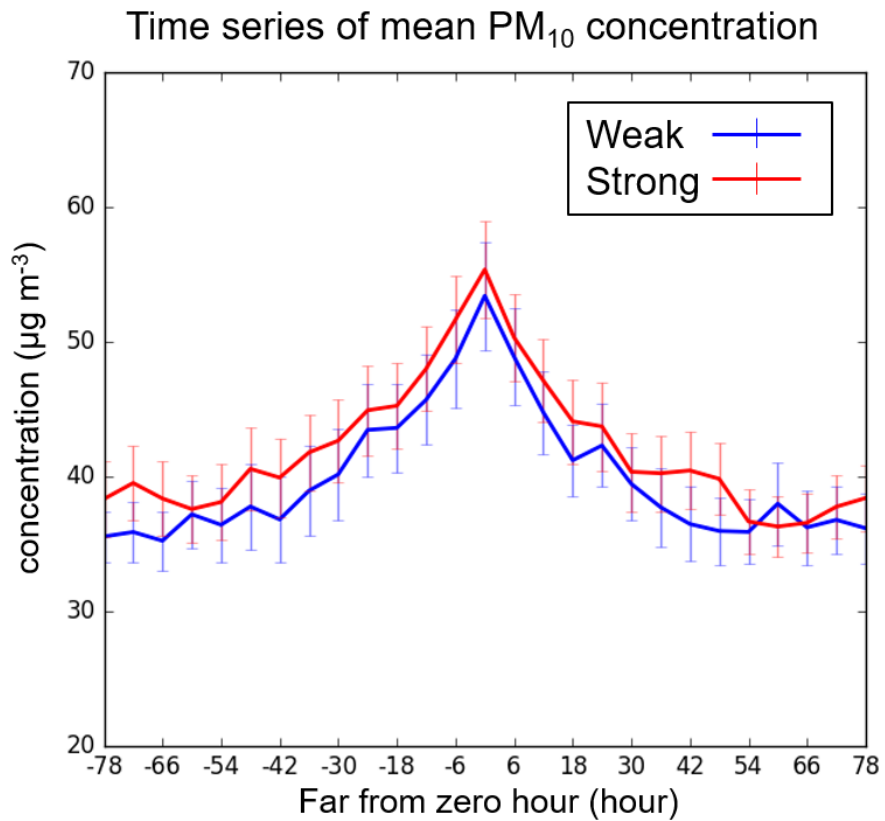


Fig. 10 Time series of mean PM₁₀ concentration of weak intensity typhoons (blue line) and strong intensity typhoon (red line). Error bars indicate 95% confidence interval.

3.2.3. *PM₁₀ source type*

In addition to the meteorological condition, the transport of PM₁₀ concentration toward South Korea should also be considered because of a locational characteristic. According to Lee et al. (2011), when high PM₁₀ pollution episode is influenced by long-range transport type, PM₁₀ concentration is the highest compared to in-between type and local type. In this regard, the type identification of the inflow of PM₁₀ aerosol is classified by using a back trajectory model, called HYSPLIT, which is commonly used for identifying transboundary transport of pollutants. The arrival date is the maximum PM₁₀ concentration date for each typhoon, and the arrival point is city, Deajeon which is considered as a center of South Korea (36.3°N, 127.4°E) at the two different heights of 500 m and 1000 m above ground level.

The back trajectory results of 219 typhoons are shown in Fig. 11a. Based on the source region information, 219 typhoons are classified into three types (local, oceanic and continental types) as Fig. 11b. The number of typhoons sorted in three groups are 64 (29.2%), 59 (27.0%) and 96 (43.8%) for local type, oceanic type and continental type, respectively. The local type can be explained as the PM₁₀ stagnation by stable and light-wind condition. In case of oceanic type, the maximum PM₁₀ concentration can be expected to be originated from local emission because the PM₁₀ emission factor is not distributed over the oceanic region. In contrary, there are many severe PM₁₀ source regions in China which can expect to transport PM₁₀ aerosols from high concentration region.

For the reason of the somewhat subjective classification, time series of mean PM₁₀ concentration in island Baengnyeong-do (35.57°N, 124.37°E) which is located in the West Sea and Seoul is analyzed to identify whether transport of PM₁₀

appears only in continental type (Lim et al., 2013). Only in the group of continental type showed 1day lag of peak mean PM_{10} concentration in Seoul after appearing PM_{10} concentration peak in the island Baengnyeong-do. Based on this result, the classification according to the HYSPLIT results may be considered to be done well, and further composite analysis is conducted.

The results of composite analysis of 500 hPa geopotential anomaly, boundary layer height and 850 hPa temperature anomaly for three source types show the wave train propagated from the SCS only except the continental type (Fig. 12a, d and g). The amplitude of wave train in oceanic type is stronger than the local type. The center of high pressure anomaly system is located between South Korea and Japan (Fig. 12a and d), and according to the composite of boundary layer height anomaly, significantly anomalous low boundary layer height is distributed around South Korea (Fig. 12b and e). In contrary, boundary layer height in the continental type shows anomalously high around South Korea (Fig. 12h).

In the composite temperature anomaly of local and oceanic types, anomalous warm conditions are seen in the both types. However, in the continental type, there is anomalous cold condition is over South Korea which is not favorable condition for chemical reaction (Fig. 12c, f and i). This can be referred as the influence of typhoon on PM_{10} concentration in South Korea by the Rossby wave propagation is appeared as local PM_{10} factors which is appeared as local and oceanic type. Additionally, when continental type of PM_{10} is transported, Rossby wave propagation is not well detected.

The PM_{10} concentration in entire period, the continental type is the most the highest, followed by the local type and the oceanic type. The PM_{10} concentration is significantly different near zero hour. According to previous analysis, in the

continental type, as the Rossby wave propagation does not clearly appear in the composite field, typhoon influence by Rossby wave propagation is not absolute.

The local and oceanic type have typhoons which are occurred in summer for 34 (53.1%) and 44 (74.6%), respectively, and the number of typhoons in autumn 29 (45.3%) and 13 (22.0%), respectively. The typhoons generated in summer is dominant for both groups. On the contrary, the continental type dominantly has typhoons in autumn having 28 typhoons (29.2%) in summer and 50 typhoons (52.1%) in autumn. The seasonal difference on propagation of Rossby wave by typhoon in the SCS is affected in difference of groups.

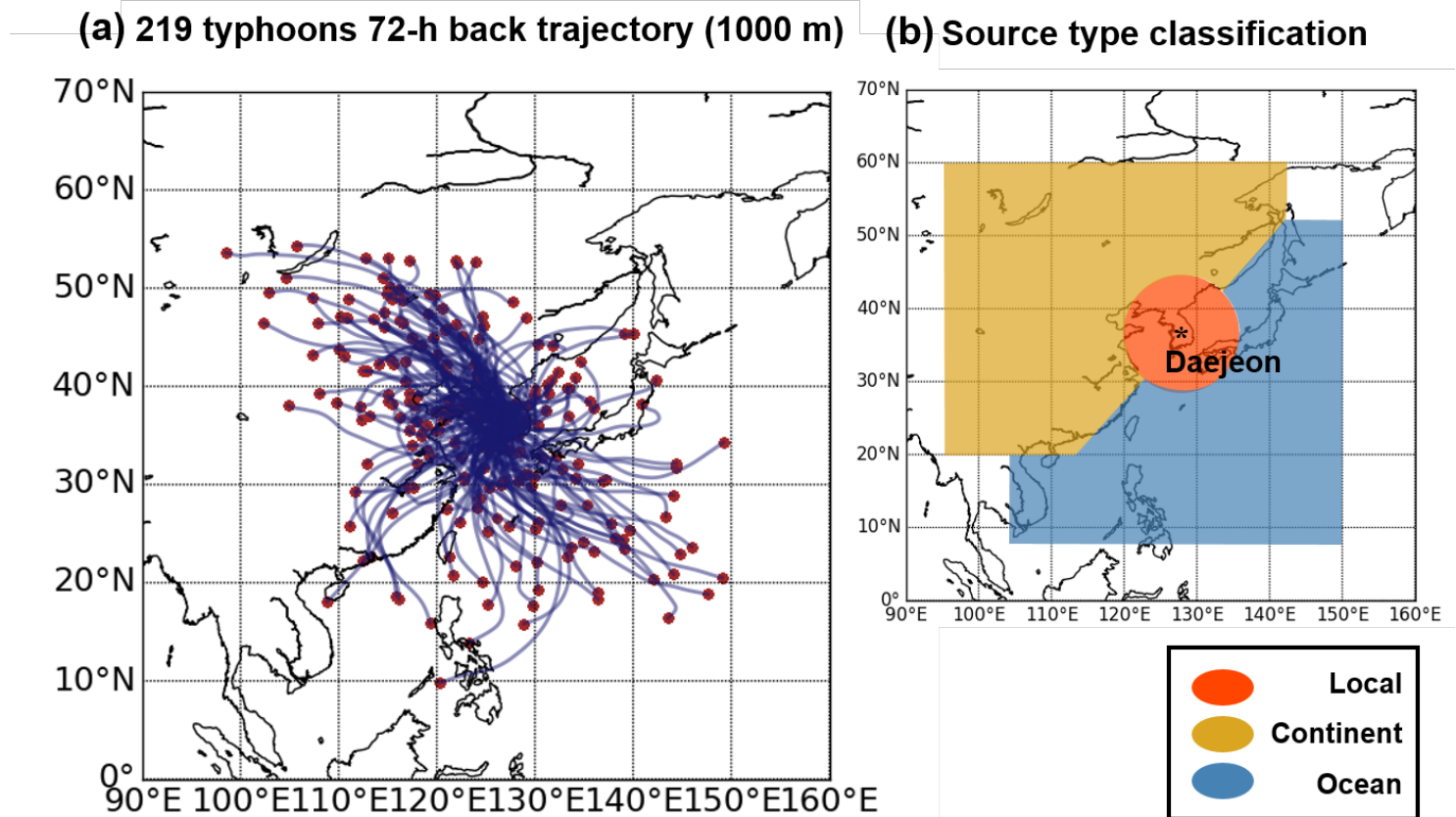


Fig. 11. (a) The 72-h back trajectory in 1000 m from surface, originating in Deajeon, produced by HYSPLIT model. (b) Distribution of area for classification of source types.

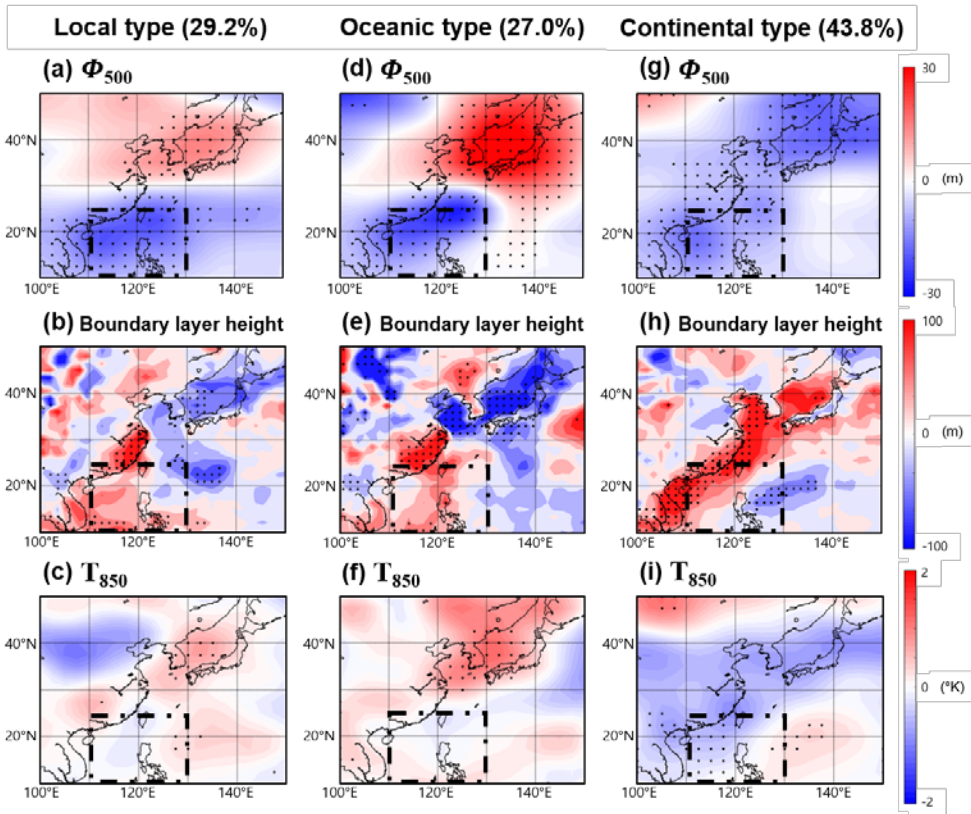


Fig. 12. Composites of 500 hPa geopotential height anomaly (Φ_{500} (a), (d) and (g)), the boundary layer height ((b), (e) and (h)) and anomaly 850 hPa air temperature (T_{850} , (c), (f) and (i)). The left, middle, and right panels are the local, oceanic, and continental type, respectively. Dots indicate grids with the 90% statistical significance based on a t-test. Square boxes indicate the SCS.

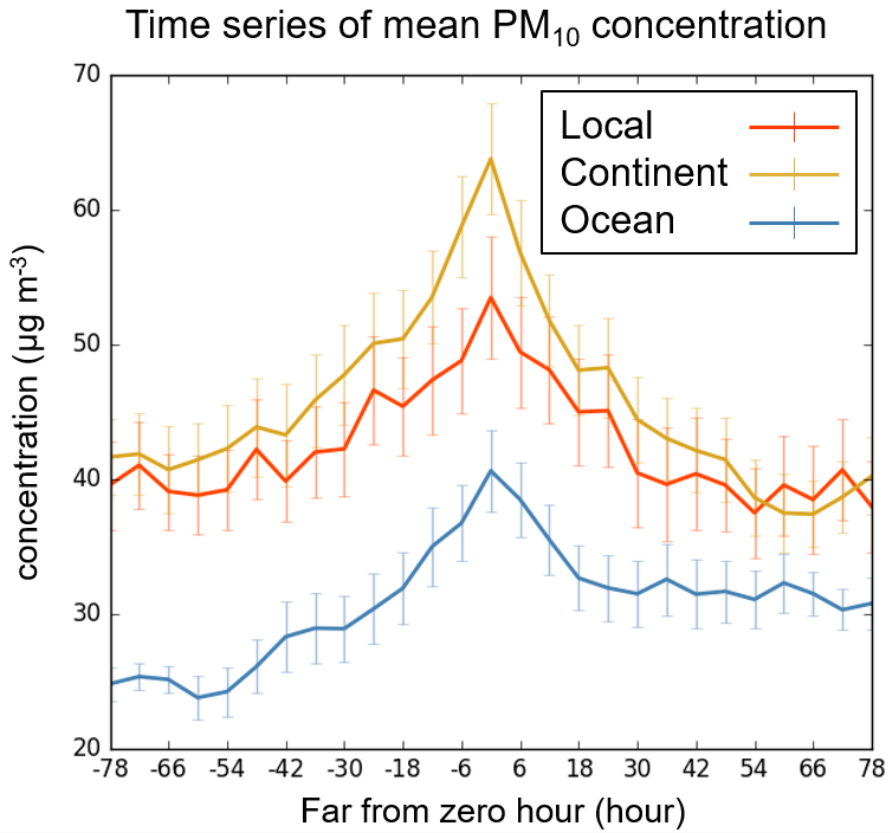


Fig. 13. Time series of mean PM₁₀ concentration of typhoons for local source type (red line), the continental type (orange line) and the oceanic type (blue line). Error-bars indicate 95% confidence interval.

3.2.4. *Combination of environmental conditions*

For now, we investigate the influence of typhoon on variation of PM₁₀ concentration in South Korea according to various factors which are season, typhoon intensity and the source type of PM₁₀, and analyze the characteristic of background condition and temporal mean PM₁₀ concentration through the composite analysis. Based on the previous classification results, 219 typhoons can be sorted into more detailed groups (Table 1).

According to the result in Table 1, the group of typhoons that has the highest PM₁₀ concentration increase (26.4 $\mu\text{g m}^{-3}$) is the strong typhoons in autumn under the influence of continental PM₁₀ source type that contains 28 typhoons. However, according to the analysis in 3.2.3., the Rossby wave propagation is not clear in the 500 hPa geopotential height anomaly field for the continental source type. Based on the above information, to consider the influence of typhoons in the SCS, we do not consider the groups sorted by the continental type.

The most increased PM₁₀ concentration from seasonal mean is 17.2 $\mu\text{g m}^{-3}$ in the typhoon group which have strong intensity and are affected by local emission in autumn season. It contains 21 typhoons and average of the maximum PM₁₀ concentration is 54.9 $\mu\text{g m}^{-3}$. In contrast, the lowest concentration increase (-5.3 $\mu\text{g m}^{-3}$) appears in the group of strong typhoons in summer experiencing oceanic wind flow. When we consider the total average PM₁₀ concentration of South Korea (50.8 $\mu\text{g m}^{-3}$), 54.9 $\mu\text{g m}^{-3}$ is higher than average and is higher than the average concentration in summer (40.9 $\mu\text{g m}^{-3}$).

Table 1. Classification of typhoons and the average of maximum PM₁₀ concentration and seasonal PM₁₀ concentration anomaly for each group. Red (Blue) color denotes group of the most PM₁₀ concentration increased (decreased) group.

Season	Typhoon intensity	Source type	# of typhoon	Average PM ₁₀ ($\mu\text{g m}^{-3}$)	* ΔPM_{10} ($\mu\text{g m}^{-3}$)
Summer	Strong	Local	15	57.5	12.3
		Continental	12	57.4	12.2
		Oceanic	24	39.9	-5.3
	Weak	Local	19	50.3	5.1
		Continental	16	66.9	21.7
		Oceanic	20	43.4	-1.8
Autumn	Strong	Local	21	54.9	17.2
		Continental	28	64.1	26.4
		Oceanic	7	35.1	-2.6
	Weak	Local	8	50.4	12.7
		Continental	22	59.2	21.5
		Oceanic	6	38.0	0.3

*Average of PM₁₀ concentrations in summer and autumn are 45.2 $\mu\text{g m}^{-3}$ and 37.7 $\mu\text{g m}^{-3}$, respectively.

4. Summary

This study investigates the climatological relationship between typhoon in the Western North Pacific and variation of PM_{10} concentration in South Korea. Among 345 typhoons that generated from 2001 to 2016, when PM_{10} concentration shows peak in South Korea during the typhoon life time, typhoon locations are most highly (more than 20% of typhoons) gathered in the SCS (110°E –130°E, 10°N – 25°N). To investigate the influence of typhoons in SCS on PM_{10} concentration in South Korea, 63.5% (219) typhoons passing through the SCS are investigated (Fig. 4a). From the composite results of geopotential height, wave train which is generated by typhoons from the SCS to the Kamchatka peninsula can be seen (Fig. 5a –c). Additionally, high pressure anomaly system from propagated wave train is located over South Korea that makes favorable conditions with anomalous warm temperature and low boundary layer height to accumulate PM_{10} concentration.

Wave propagation is strongly dependent phenomena to seasons and typhoon intensity which is trigger of generation of the wave train. Grouping analysis according to season and typhoon intensity is conducted. As results, the amplitude of wave train is stronger when typhoons in the SCS generated in summer season (Fig. 7a) and have strong intensity (Fig. 9a). However, the feature of Rossby wave propagation with high pressure system over South Korea is not clear in autumn (Fig. 7b) and for the weak typhoon intensity in the SCS (Fig. 9b). PM_{10} concentration in autumn and strong typhoon intensity group show higher concentration than the summer and weak typhoon, respectively (Fig. 8 and Fig. 10).

PM_{10} concentration is modulated not only by meteorological condition but also by the inflow of various source region. Using HYSPLIT model, 219 typhoons are

sorted into three different source types; local, continental and oceanic type. In the group of local and oceanic group, the wave train are seen in the composite of geopotential height (Fig. 12a and d). However, in composite of continental type, high pressure anomaly system appears over South Korea (Fig. 12g). Additionally, because of the anomalous high pressure system over South Korea produced by Rossby wave propagated from typhoon in SCS, meteorological data show favorable conditions to PM₁₀ stagnation which are low boundary layer height and warm temperature in the local and oceanic groups (Fig. 12b, e, c and f). However, in the continental type, high boundary layer and cold temperature anomaly around South Korea are significant.

According to the analysis so far, more detailed classification by the seasons, typhoon intensity and PM₁₀ source types is conducted (Table 1). As a result, the highest increase of PM₁₀ concentration (17.2 $\mu\text{g m}^{-3}$) influenced the Rossby wave propagation (; except continental source type) occurs in the group of typhoons that are generated in autumn, have strong typhoon intensity and under the local source type.

5. Discussion

The typhoon intensity and source type are seasonally impacted standards. Additionally, they are closely correlated to each other. For this reason, it is hard to declare which is the most significant factor to influence variation of PM₁₀ concentration in South Korea. Furthermore, the other factors that are not considered in this research is still left; precipitation, chemical formation, emission, etc. For this reason, factor quantification is furtherly needed.

The meteorological condition change due to the Rossby wave propagation by typhoon and convective system in the South China Sea and the Philippine Sea gives an influence to not only South Korea, but also to Japan. This study investigates variation of PM₁₀ concentration in South Korea only, however, the variation of PM₁₀ concentration in Japan needs to be investigated also. Additionally, the meteorological conditions which are favorable to PM₁₀ stagnation, other major pollutants like NO_x, CO, SO_x, O₃ and PM_{2.5} also doubt to be influenced. Therefore, variation of other pollutants needs to be analyzed.

Generally, the typhoon influence on PM₁₀ concentration is not indirect, but the direct when typhoons approach closely to South Korea. The direct influence of typhoon on PM₁₀ concentration in South Korea is not fully investigated, therefore the direct effect of typhoon needs to be furtherly investigated.

References

- 김정수, 2009, 태풍의 사회경제적 영향에 관한 워크숍-태풍시즌동안 대기 질 변동과 개선 효과, 기상청 세미나.
- Choi, W., Ho, C. H., Kim, J., Kim, H. S., Feng, S., & Kang, K. (2016). A track pattern-based seasonal prediction of tropical cyclone activity over the North Atlantic. *Journal of Climate*, 29(2), 481-494.
- Fang, G.-C., Lin, S.-J., Chang, S.-Y., & Chou, C.-C. (2009). Effect of typhoon on atmospheric particulates in autumn in central Taiwan. *Atmospheric Environment*, 43(38), 6039–6048.
- Feng, Y., Wang, A., Wu, D., & Xu, X. (2007). The influence of tropical cyclone Melor on PM 10 concentrations during an aerosol episode over the Pearl River Delta region of China: Numerical modeling versus observational analysis. *Atmospheric Environment*, 41(21), 4349–4365.
- Ho, C. H., Baik, J. J., Kim, J. H., Gong, D. Y., & Sui, C. H. (2004). Interdecadal changes in summertime typhoon tracks. *Journal of Climate*, 17(9), 1767-1776.
- Holst, J., Holst, T., Sähn, E., Klingner, M., Anke, K., Ahrens, D., & Mayer, H. (2009). Variability of PM10 concentrations dependent on meteorological conditions. *International Journal of Environment and Pollution*, 36, 3–18.
- Huang, J.-P., Fung, J. C., Lau, A. K., & Qin, Y. (2005). Numerical simulation and process analysis of typhoon-related ozone episodes in Hong Kong. *Journal of Geophysical Research: Atmospheres*, 110(D5). Retrieved from <http://onlinelibrary.wiley.com/doi/10.1029/2004JD004914/full>
- Jeon, B., (2011). Sudden rise of fine particle concentration after Typhoon USAGI

- and NARI passage in Busan, *Journal of Environmental Impact Assessment*, 20(4), 557–564.
- Jiang, Y. C., Zhao, T. L., Liu, J., Xu, X. D., Tan, C. H., Cheng, X. H., ... Zhao, S. Z. (2015). Why does surface ozone peak before a typhoon landing in southeast China? *Atmospheric Chemistry and Physics*, 15(23), 13331–13338.
- Kawamura, R., & Ogasawara, T. (2006). On the Role of Typhoons in Generating PJ Teleconnection Patterns over the Western North Pacific in Late Summer. *SOLA*, 2, 37–40. <https://doi.org/10.2151/sola.2006-010>
- Kim, D., Jin, C.-S., Ho, C.-H., Kim, J., & Kim, J.-H. (2015). Climatological features of WRF-simulated tropical cyclones over the western North Pacific. *Climate Dynamics*, 44(11–12), 3223–3235. <https://doi.org/10.1007/s00382-014-2410-3>
- Kosaka, Y., & Nakamura, H. (2006). Structure and dynamics of the summertime Pacific–Japan teleconnection pattern. *Quarterly Journal of the Royal Meteorological Society*, 132(619), 2009–2030. <https://doi.org/10.1256/qj.05.204>
- Kosaka, Y., Xie, S.-P., & Nakamura, H. (2011). Dynamics of Interannual Variability in Summer Precipitation over East Asia. *Journal of Climate*, 24(20), 5435–5453. <https://doi.org/10.1175/2011JCLI4099.1>
- Kurihara, K., & Tsuyuki, T. (1987). Development of the Barotropic High around Japan and its Association with Rossby Wave-like Propagations over the North Pacific: Analysis of August 1984. *Journal of the Meteorological Society of Japan. Ser. II*, 65(2), 237–246. https://doi.org/10.2151/jmsj1965.65.2_237
- Lam, Y. F., Cheung, H. M., & Ying, C. C. (2018). Impact of tropical cyclone track change on regional air quality. *Science of The Total Environment*, 610–611(Supplement C), 1347–1355.

<https://doi.org/10.1016/j.scitotenv.2017.08.100>

- Lee, S., Ho, C.-H., & Choi, Y.-S. (2011). High-PM10 concentration episodes in Seoul, Korea: Background sources and related meteorological conditions. *Atmospheric Environment*, 45(39), 7240–7247. <https://doi.org/10.1016/j.atmosenv.2011.08.071>
- Lee, S., Ho, C.-H., Lee, Y. G., Choi, H.-J., & Song, C.-K. (2013). Influence of transboundary air pollutants from China on the high-PM10 episode in Seoul, Korea for the period October 16–20, 2008. *Atmospheric Environment*, 77(Supplement C), 430–439. <https://doi.org/10.1016/j.atmosenv.2013.05.006>
- Lim, D. Y., Lee, T. J., & Kim, D. S. (2012). Quantitative Estimation of Precipitation Scavenging and Wind Dispersion Contributions for PM 10 and NO 2 Using Long-term Air and Weather Monitoring Database during 2000~ 2009 in Korea. *Journal of Korean Society for Atmospheric Environment*, 28(3), 325-347.
- MacNee, W., & Donaldson, K. (2003). Mechanism of lung injury caused by PM10 and ultrafine particles with special reference to COPD. *The European Respiratory Journal. Supplement*, 40, 47s–51s.
- Medina-Ramón, M., Zanobetti, A., & Schwartz, J. (2006). The Effect of Ozone and PM10 on Hospital Admissions for Pneumonia and Chronic Obstructive Pulmonary Disease: A National Multicity Study. *American Journal of Epidemiology*, 163(6), 579–588. <https://doi.org/10.1093/aje/kwj078>
- Nitta, T. (1987). Convective Activities in the Tropical Western Pacific and Their Impact on the Northern Hemisphere Summer Circulation. *Journal of the Meteorological Society of Japan. Ser. II*, 65(3), 373–390. https://doi.org/10.2151/jmsj1965.65.3_373
- Oh, H.-R., Ho, C.-H., Kim, J., Chen, D., Lee, S., Choi, Y.-S., ... Song, C.-K. (2015).

- Long-range transport of air pollutants originating in China: a possible major cause of multi-day high-PM 10 episodes during cold season in Seoul, Korea. *Atmospheric Environment*, *109*, 23–30.
- Park, Y. M., Park, K. S., Kim, H., Yu, S. M., Noh, S., Kim, M. S., ... & Kim, Y. H. (2018). Characterizing isotopic compositions of TC-C, NO₃-N, and NH₄⁺-N in PM 2.5 in South Korea: Impact of China's winter heating. *Environmental Pollution*, *233*, 735-744.
- Takaya, K., & Nakamura, H. (2001). A formulation of a phase-independent wave-activity flux for stationary and migratory quasigeostrophic eddies on a zonally varying basic flow. *Journal of the atmospheric sciences*, *58*(6), 608-627.
- Van der Wal, J. T., & Janssen, L. H. J. M. (2000). Analysis of spatial and temporal variations of PM 10 concentrations in the Netherlands using Kalman filtering. *Atmospheric Environment*, *34*, 3675–3687. [https://doi.org/10.1016/S1352-2310\(00\)00085-6](https://doi.org/10.1016/S1352-2310(00)00085-6)
- Wang, G., Huang, L., Gao, S., Gao, S., & Wang, L. (2002). Characterization of water-soluble species of PM₁₀ and PM_{2.5} aerosols in urban area in Nanjing, China. *Atmospheric Environment*, *36*(8), 1299–1307. [https://doi.org/10.1016/S1352-2310\(01\)00550-7](https://doi.org/10.1016/S1352-2310(01)00550-7)
- Wang, X., Wang, Z., Yu, T., & Gong, Y. (2009). Foreshowing of the Western Pacific tropical cyclone track to PM₁₀ air pollution episode in the Beijing area. *Chinese Science Bulletin*, *54*(5), 830–835.
- Wu, M., Wu, D., Fan, Q., Wang, B. M., Li, H. W., & Fan, S. J. (2013). Observational studies of the meteorological characteristics associated with poor air quality over the Pearl River Delta in China. *Atmospheric Chemistry and Physics*, *13*(21), 10755–10766.

- Yan, J., Chen, L., Lin, Q., Zhao, S., & Zhang, M. (2016). Effect of typhoon on atmospheric aerosol particle pollutants accumulation over Xiamen, China. *Chemosphere*, *159*, 244–255.
- Yang, J. X., Lau, A. K. H., Fung, J. C. H., Zhou, W., & Wenig, M. (2012). An air pollution episode and its formation mechanism during the tropical cyclone Nuri's landfall in a coastal city of south China. *Atmospheric Environment*, *54*(Supplement C), 746–753. <https://doi.org/10.1016/j.atmosenv.2011.12.023>
- Zhao, H., Che, H., Zhang, X., Ma, Y., Wang, Y., Wang, H., & Wang, Y. (2013). Characteristics of visibility and particulate matter (PM) in an urban area of Northeast China. *Atmospheric Pollution Research*, *4*(4), 427–434. <https://doi.org/10.5094/APR.2013.049>

국문 초록

이 학위 논문은 북서태평양의 태풍과 한국 PM_{10} 농도 변화 간의 기후학적 관계를 조사한 것이다. 2001년부터 2016년에 발생한 219 개의 태풍 중 26%의 태풍이 각 태풍 생애 기간 중의 최대 PM_{10} 농도가 나타났을 때 남중국해 (SCS; $110^{\circ}E - 130^{\circ}E$ and $10^{\circ}N - 25^{\circ}N$) 에 위치하고 있음을 알 수 있었다. SCS를 지나는 219개의 태풍의 SCS를 지날 때 컴퍼짓 분석을 통하여, SCS로부터 캄차카 반도까지 이어지는 로스비파 형태의 패턴이 보이는 것을 알 수 있었다. 로스비파의 전파는 한반도 주변에 아노말리 고기압과 낮은 경계층 높이, 아노말리하게 높은 온도의 조건을 만족시키면서 PM_{10} 의 농축에 유리한 환경을 조성하였다. 또한, 로스비파의 패턴은 계절과 태풍의 세기 특성에 따라서 크게 달랐다. 로스비파의 진폭은 가을철에 비하여 여름철에 강했으며 강한 태풍이 SCS에 위치할 경우가 약한 태풍이 SCS에 위치할 때에 비하여 진폭이 강했다. 또한, 가을철 PM_{10} 농도가 여름철에 비하여 높았고, 강한 태풍이 SCS에 위치할 경우에 PM_{10} 농도가 더 높은 것으로 나타났다. 반면에, 한국 PM_{10} 농도를 고려할 때 유입 경로에 대한 분석 또한 로스비파의 분석만큼 중요하므로, 역궤적 모델인 HYSPLIT을 이용한 72 시간 역궤적을 산출하여 219 개의 태풍을 국내 요인, 서대륙 유입 그리고 동해 유입의 세 그룹으로 나누어 배경 특성을 분석하였다. 국내 요인과 동해 유입의 두 그룹에 대하여 기압 패턴의 컴퍼짓 분석 결과에 로스비파의 형태가 나타났으나 서대륙 유입의 경우에는 로스비파의

형태가 나타나지 않았다. 또한, 국내 요인과 동해 유입의 그룹에서는 한국 주변이 낮은 경계층 높이와 850 hPa의 높은 아노말리 온도를 보이며 PM₁₀의 농축에 유리한 조건을 만족했음을 알 수 있었다. 서대륙 유입의 경우에는 PM₁₀ 농축에 유리한 조건이 나타나지 않은 것을 확인할 수 있었다. 세 그룹에 대하여 PM₁₀ 농도는 서대륙 유입의 경우가 가장 높았으며 그 뒤를 국내 요인, 동해안 유입이 따랐다. 위 분석을 토대로 계절, 태풍 세기, 그리고 PM₁₀ 유입 경로에 대하여 12개의 그룹으로 나누어 살펴 본 결과, 로스비파의 영향으로 계절 평균에 대하여 가장 높은 PM₁₀의 증가 (17.15 $\mu\text{g m}^{-3}$)를 경험했던 태풍 그룹 (21개의 태풍을 포함)의 조건은 가을철 강한 태풍이 SCS에 위치하면서 국내 요인으로 인하여 증가한 경우인 것으로 나타났다. 다음의 분석을 통하여 화자는 한국 PM₁₀ 농도의 변화에 남중국해에 위치한 태풍이 부분적으로 영향을 줄 수 있으며, PM₁₀ 농도를 고려할 때에 태풍의 요인 또한 고려되어야 할 필요성을 제시한다.

주요 용어: PM₁₀ 농도, 태풍, 남중국해, 로스비파 전파, 계절성, 태풍 세기,

PM₁₀ 유입 경로, HYSPLIT

학 번: 2016-20434